Single-trial EEG classification of motor imagery using deep convolutional neural networks
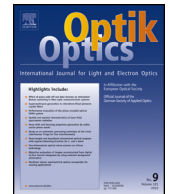
3 authors, including:

Some of the authors of this publication are also working on these related projects:

Gait Recognition View project

Deep Learning Applications View project

Original research article

Single-trial EEG classification of motor imagery using deep convolutional neural networks

Zhichuan Tang [a,b,*], Chao Li [b], Shouqian Sun [b]

[a] Industrial Design Institute, Zhejiang University of Technology, Hangzhou 310023, China
[b] College of Computer Science and Technology, Zhejiang University, Hangzhou 310027, China

ARTICLE INFO

ABSTRACT

Electroencephalogram (EEG) signal recorded during motor imagery (MI) has been widely applied in non-invasive brain–computer interface (BCI) as a communication approach. In this paper, we propose a new method based on the deep convolutional neural network (CNN) to perform feature extraction and classification for single-trial MI EEG. Firstly, based on the spatio-temporal characteristics of EEG, a 5-layer CNN model is built to classify MI tasks (left hand and right hand movement); then the CNN model is applied in the experimental data set collected from subjects, and compared with other three conventional classification methods (power + SVM, CSP + SVM and AR + SVM). The results demonstrate that CNN can further improve classification performance: the average accuracy using CNN ($86.41 \pm 0.77\%$) is 9.24%, 3.80% and 5.16% higher than those using power + SVM, CSP + SVM and AR + SVM, respectively. The present study shows that the proposed method is effective to classify MI, and provides a practical method by non-invasive EEG signal in BCI applications.

© 2016 Elsevier GmbH. All rights reserved.

1. Introduction

Brain–computer interfaces (BCI) based on electroencephalogram (EEG) have received a huge interest as a direct communication pathway between a human brain and an external device [1–3]. The non-invasive recording procedure is safe and easy to apply, and it is potentially applicable to almost all people including those seriously amputated and paralyzed patients [4–6].

Motor imagery (MI) has been widely applied in non-invasive BCI as a communication approach [7]. When human imagines or executes the movement of unilateral limb, the power of mu and beta rhythms will decrease or increase in the sensorimotor area of the contralateral hemisphere and the ipsilateral hemisphere, respectively [8,9]. The former case is called event-related desynchronization (ERD), and the latter is event-related synchronization (ERS) [10]. The ERD/ERS patterns can be utilized as important features in the discrimination between right hand and left hand movement, or hand and foot movement.

Pattern recognition techniques are used for the classification and the detection of MI. In the conventional classification methods, firstly the hand-designed input features are extracted, and then the machine learning algorithms are used to build a mapping between EEG features and MI [11,12]. However, the separation of two modules (feature extraction and classification) may result in the information loss during the feature extraction process [13]. Besides, the low signal-noise

* Corresponding author at: Industrial Design Institute, Zhejiang University of Technology, Hangzhou 310023, China.
E-mail addresses: ttzzcc@zju.edu.cn (Z. Tang), superli@zju.edu.cn (C. Li), ssq@zju.edu.cn (S. Sun).

ratio of EEG signal can affect classification accuracy. Therefore, in some previous studies using conventional methods, the MI classification accuracies were lower than 80% [14,15].

Convolutional neural networks (CNN) are biologically-inspired variants of multilayer perceptron (MLP) designed to use minimal amounts of preprocessing [16]. They have wide applications in image and video recognition [17], and natural language processing [18]. Based on the receptive field and weight sharing, the complexity of the network structure is reduced, i.e., the number of weights is reduced. Due to directly face to the raw signal, it helps to extract the most discriminant features (high-level features) for classification. Some researchers have used CNN for feature extraction and classification of event-related potential (ERP). Hubert et al. [19] proposed a CNN-based method to detect P300 wave, and the results showed a highest classification accuracy of 95% on a data set of the BCI competition. The previous study indicated that CNN seems to be a good approach for EEG signals classification. However, ERP belongs to evoked potential, while MI belongs to spontaneous EEG, which leads to different performances and modes. For now, few studies focused on the MI classification using CNN.

In this paper, we propose a new method based on the deep convolutional neural network (CNN) to perform feature extraction and classification for MI EEG signal. Firstly, based on the spatio-temporal characteristics of EEG, a 5-layer CNN model is built to classify MI tasks (left hand and right hand movement); then the CNN model is applied in the experimental data set collected from two subjects, and compared with other three conventional classification methods (power + SVM, CSP + SVM and AR + SVM).

The remaining of this paper is organized as follows. The materials and methods are described in Section 2. Then the experimental results and discussion are presented in Section 3. Finally, the conclusion is summarized in Section 4.

2. Materials and methods

2.1. Data acquisition

Two able-bodied subjects participated in this study. They were all right handed according to the Edinburgh inventory [20], and none of them had been exposed to a BCI system or informed of the experimental hypothesis. The experimental protocol was reviewed and approved by the human ethical clearance committee of Zhejiang University. Informed written consent was obtained from all subjects that volunteered to perform this experiment.

EEG data were recorded from 28 active electrodes (FC5, FC3, FC1, FCz, FC2, FC4, FC6, C5, C3, C1, Cz, C2, C4, C6, CP5, CP3, CP1, CPz, CP2, CP4, CP6, P5, P3, P1, Pz, P2, P4, P6) attached on an EEG cap in conjunction with the ActiveTwo 64-channel EEG system (BioSemi B.V., Amsterdam, Netherlands). This system replaces the ground electrodes in conventional systems with two separate electrodes (CMS and DRL). The reference electrode was placed on the left mastoid. Fig. 1 shows the location of the electrodes. EEG was sampled at 1000 Hz, power-line notch filtered at 50 Hz, and band-pass filtered at between 0.5 and 100 Hz. Before electrode attachment, alcohol was used to clean the skin, and conductive gel was used to reduce electrode resistance.

2.2. Experiment procedure

Subjects were seated in a comfortable chair, and were asked to avoid eye movements, blinks or swallowing during the visual cue onset, as shown in Fig. 2. They were instructed to perform two classes MI, i.e., left hand movement or right hand movement. Each subject completed totally 460 trials, consisting of random sequences of 230 trials of two classes MI. As shown in Fig. 3, each trial started with the presentation of an acoustical warning tone and a cross (second 2). One second later, a cue was randomly chosen in one of two ("←" and "→"), which indicated the movement to be imagined. After cue
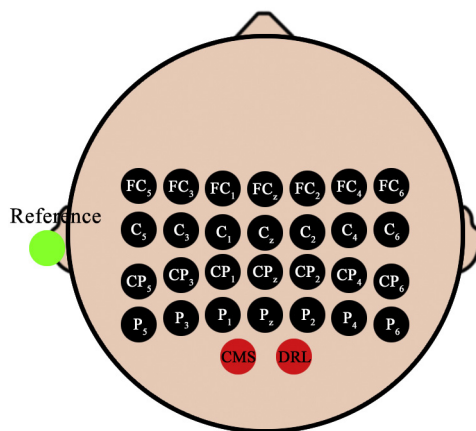

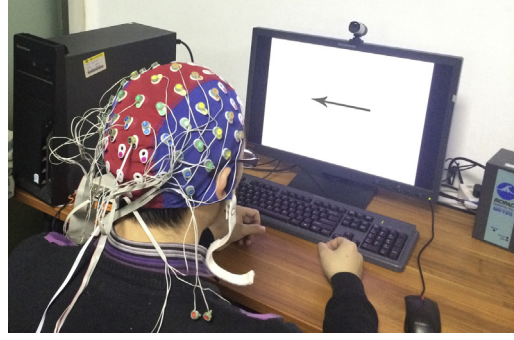**Fig. 1.** Location of the electrodes.

Fig. 2. Experimental setup. Subjects were instructed to perform two classes MI, i.e., left hand movement or right hand movement. The left arrow indicated left hand MI, the right arrow indicated right hand MI.

was presented, subjects had to perform the MI for 5 s, until the screen content was erased (second 8). After a short pause (random duration between 2 and 5 s) the next trial started.

2.3. Data preprocessing

The raw EEG signal was filtered in an 8–30 Hz band. The frequency band was chosen because it includes the alpha and beta frequency bands, which have been shown to be most important for movement classification [15]. To show the ERD/ERS of each class (left hand movement and right hand movement), the EEG signals of C3, Cz and C4 channels were averaged online over the 3 s preceding and 5 s following cue appearance across all trials and all subjects. ERD/ERS is defined as the percentage of power decrease or power increase in relation to a reference period (in this study 0–1 s), according to the expression

$$\frac{ERD}{ERS}\% = \frac{EEG_A - EEG_R}{EEG_R} \times 100\% \tag{1}$$

where A is the power of the interest period, and R is the power of the reference period. ERD/ERS visualizations were created by generating time-frequency maps using a fast Fourier transformation (FFT). According to the visual inspection of ERD and ERS (refer to Figs. 5 and 6 in Section 3), the time period 1–4 s after the cue appearance (second 4–7) and the best frequency band for each subject were selected in order to obtain the strongest ERD/ERS to extract features. Each selected time period was analyzed using time segments of 50 ms. Therefore, the input of the CNN was a matrix $28(N) \times 60(T)$, where N is the number of channels, and T is the number of points that are considered for the analysis: $T = 3\,\text{s}(time\ period) \times 1000\,\text{Hz} \div 50\,\text{ms}(window)$.

2.4. CNN topology

Based on the spatio-temporal characteristics of EEG, a 5-layer CNN model was constructed, as shown in Fig. 4. The first layer (L1) is the input layer; the second (C2) and third layers (C3) are hidden layers, which compose the feature extraction part; the output of C3, and the forth and fifth layers compose the classification part. In the proposed CNN model, the convolution kernels are not matrix which is used in image recognition, but vectors. The reason is to not mix the space and time domain information in one kernel feature. The network topology is described as follows:

(1) L1: The input layer. The input is a 28×60 matrix.
(2) C2: The convolutional layer (first hidden layer). This layer aims at filtering the EEG signal in the space domain. 8 spatial filters are used in this layer, after convolution operation, 8 feature maps are obtained. The convolution kernel has a size of $[28 \times 1]$, and the each feature map has a size of (1×60).
(3) C3: The convolutional layer (second hidden layer). This layer aims at subsampling and transforming the EEG signal in the time domain. For each feature map in C2, 5 filters are used resulting in totally 40 feature maps in C3. The convolution
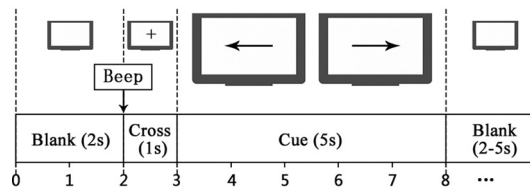

Fig. 3. Timing of one trial used in the experiment. Each trial started with the presentation of an acoustical warning tone and a cross (second 2). One second later, a cue was randomly chosen in one of two ("←" and "→"), which indicated the movement to be imagined. After cue was presented, subjects had to perform MI for 5 s, until the screen content was erased (second 8). After a short pause (random duration between 2 and 5 s) the next trial started.
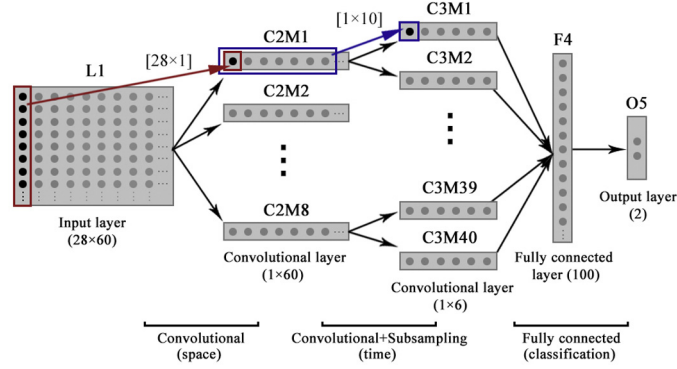
Fig. 4. 5-Layer CNN architecture for MI classification.

kernel has a size of $[1 \times 10]$, and the each feature map has a size of (1×6). This layer transforms the signal of 60 values into 6 new values in C3. According to an identical linear transformation, the size of the EEG signal is reduced to 6 neurons of each feature map.

(4) F4: The fully connected layer (third hidden layer). Each neuron of f4 is connected to each neuron of C3. C3 and F4 are fully connected. This layer is composed of 100 neurons.

(5) O5: The output layer. This layer has only two neurons, which represents the two classes of the problem (left hand movement and right hand movement). This layer is fully connected to F4.

2.5. CNN learning

A neuron in the CNN is defined by $n(l, m, j)$, where l is the layer, m is the feature map, and j is the position in this feature map. The input and output of each neuron can be represented by $x_m^l(j)$ and $y_m^l(j)$, and

$$y_m^l(j) = f\left(x_m^l(j)\right) \tag{2}$$

where $f()$ is the activation function. The hyperbolic tangent function is used as activation function for the first two hidden layers (C2 and C3):

$$f(x) = a \tanh(bx) \tag{3}$$

where $a = 1.7159$, and $b = 2/3$ (the constants are set according to the recommendations described in [21]). The sigmoid function is used as activation function for the two last layers:

$$f(x) = \frac{1}{1 + \exp^{-x}} \tag{4}$$

For C2 and C3, each neuron of the map shares the same set of weights. The neurons of these layers are connected to a subset of neurons from the previous layer. The information transmission between neurons of different layers is as follows:

(1) For L1: The input matrix can be represented by $I_{N,T}$.
(2) For C2: Through convolution operation and activation function, the input feature map of previous layer is transformed a output feature map:

$$y_m^2 = f\left(\sum_{i=1}^{i \leq 28} I_{i,j} \times k_m^2 + b_m^2(j)\right) \tag{5}$$

where k_m^2 is the convolution kernel of $[28 \times 1]$, and $b_m^2(j)$ is the bias.
(3) For C3: This layer is similar to C2:

$$y_m^3 = f\left(\sum_{i=1}^{i \leq 10} y_m^2[(j-1) \times 10 + i] \times k_m^3 + b_m^3(j)\right) \tag{6}$$

where k_m^3 is the convolution kernel of $[1 \times 10]$, and $b_m^3(j)$ is the bias.
(4) For F4: This layer is fully connected to C3:

$$y^4 = f\left(\sum_{i=1}^{i \leq 40} \sum_{p=1}^{p \leq 6} y_i^3(p) w_i^4(p) + b^4(j)\right) \tag{7}$$

where $w_i^4(p)$ is the weight value from neurons of C3 to F4, and $b^4(j)$ is the bias.

(5) For O5: This layer is fully connected to F4:

$$y^5 = f\left(\sum_{i=1}^{i \le 100} y^4(i)w^5(i) + b^5(j)\right) \tag{8}$$

where $w^5(i)$ is the weight value from neurons of F4 to O5, and $b^5(j)$ is the bias.

For each neuron, the input weights and the threshold are initialized with a standard distribution around $[\pm 1/N_{n(l,m,i)}^{input}]$, where $N_{n(l,m,i)}^{input}$ is the number of input of $n(l, m, i)$. The learning rate η_1 of C2 and C3 is defined by [19]

$$\eta_1 = \frac{2\lambda}{N_{n(l,m,0)}^{shared}\sqrt{N_{n(l,m,i)}^{input}}} \tag{9}$$

where $N_{n(l,m,0)}^{shared}$ is the number of neurons that share the same set of weights, and λ is a constant. The learning rate η_2 of F4 and O5 is defined by [19]

$$\eta_2 = \frac{\lambda}{\sqrt{N_{n(l,m,i)}^{input}}} \tag{10}$$

Gradient descent method is used to tune and correct the weights and bias of this CNN.

2.6. Classification

During the CNN training step, each subject's data were used to train his own classification model. The whole data set were separated into training set (80% data) and testing set (20% data). We performed the 10-fold cross-validation procedure in the model training step, i.e., 9-folds data of the training set were used for training and the remaining 1 fold data were used for validation. To compare with our proposed method, we employed other three conventional classification methods, i.e., power + SVM [22], CSP (common spatial pattern) + SVM [23] and AR (AutoRegression) + SVM [24], to train the classification models respectively using the same training set, and then these models were tested using the same testing set. Accuracy and ROC curve were used to evaluate the classification models; precision, recall and *F*-score were used to evaluate the classification performance for each class.

3. Results and discussion

3.1. ERD/ERS analysis

To show time course of ERD/ERS, for each movement (left hand and right hand movement), the EEG power of C3, Cz and C4 within 8–12 Hz frequency band is averaged offline over the 3 s preceding and 5 s following cue appearance across all trials and all subjects, and is displayed relative (as percentage) to the power of the same EEG derivations recorded during the reference period, as shown in Fig. 5. During the left hand and right hand MI (the time period 1–5 s after the cue appearance (second 4–8)), the EEG data reveals a significant ERD (second 4–7) and post-movement ERS (second 7–8) over the contralateral side,
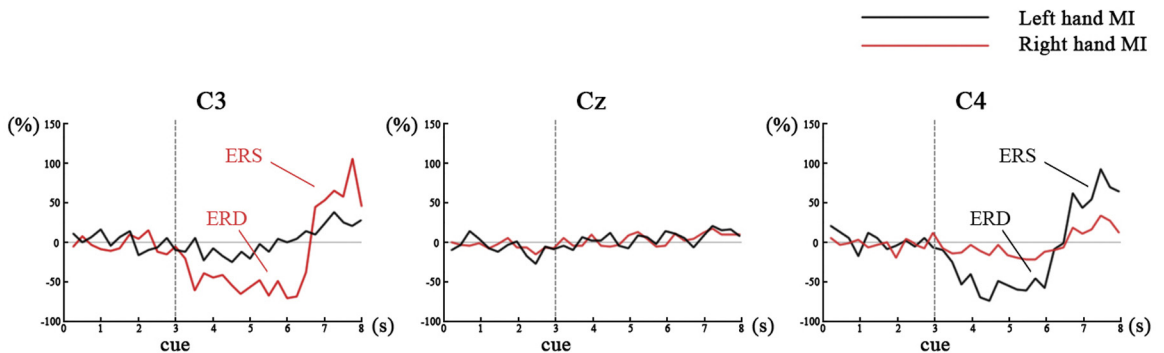

Fig. 5. Time course of ERD/ERS. For each movement (left hand and right hand), the EEG power of C3, Cz and C4 within 8–12 Hz frequency band is averaged offline over the 3 s preceding and 5 s following cue appearance across all trials and all subjects, and is displayed relative (as percentage) to the power of the same EEG derivations recorded during the reference period.
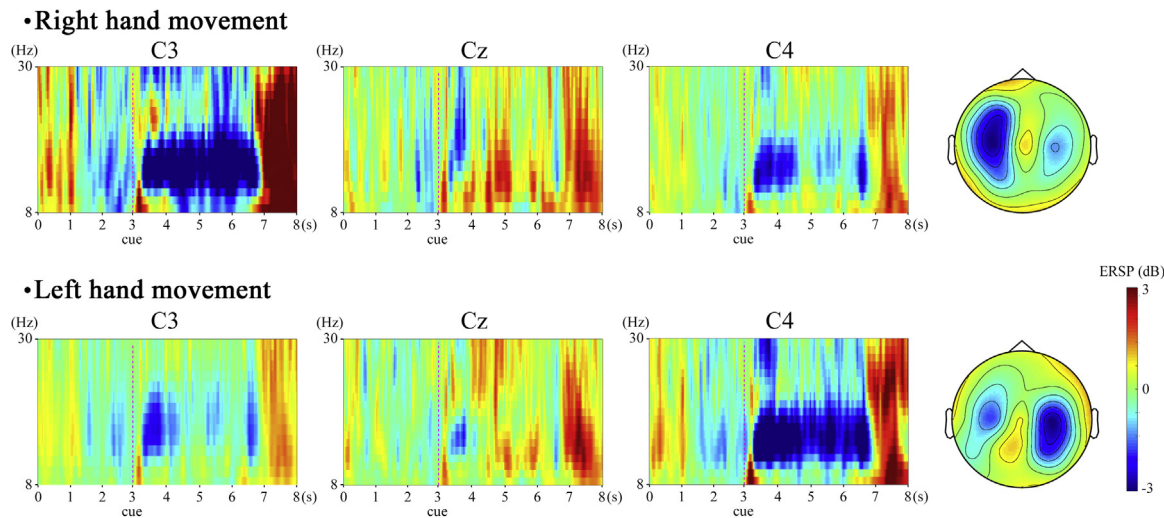
Fig. 6. A representative example of time–frequency maps of two movements from subject 2. For each movement, time–frequency maps of channel C3 over the left sensorimotor cortex, C4 over the right sensorimotor cortex and Cz are illustrated. In the time–frequency map, 3 s means the cue occurrence. Blue color stands for ERD (power decrease), and red color stands for ERS (power increase). (For interpretation of the references to color in this figure legend, the reader is referred to the web version of the article.)

while only a weak ERS can be seen over the ipsilateral side and at the Cz electrode. Therefore, the EEG data during second 4–7 were selected for classification models training.

Fig. 6 shows a representative example of time–frequency maps of two movements from subject 2. For each movement, time–frequency maps of channel C3 over the left sensorimotor cortex, C4 over the right sensorimotor cortex and Cz are illustrated. In the time-frequency map, 3 s means the cue occurrence. Blue color stands for ERD (power decrease), and red color stands for ERS (power increase). For the right hand and left hand movement, ERD is observed from around 1–4 s (second 4–7) after the cue onset due to the response delay; ERD in both alpha and beta bands is observed over motor areas contralateral to the hand moves. The ERS is mainly observed over around second 7–8 in the beta band over the contralateral motor areas. For subject 2, the time–frequency maps show that 12–16 Hz is the best frequency to obtain the strongest ERD/ERS to extract features. The head topographies corresponding to this frequency band from second 4–7 are provided next to the time–frequency maps. For subject 1, the best frequency bands are 18–22 Hz.

3.2. Classification results

During the CNN training step, each subject's data were used to train his own classification model. Besides, the other methods (power + SVM, CSP + SVM and AR + SVM) were used to train the classification models to compare with the CNN model. The confusion matrices of four methods for testing set are shown in Fig. 7. The number of each entry in the matrix represents the mean value and standard deviation across all subjects. The main diagonal entries stand for the correct classification, and the off-diagonal entries stand for the misclassification. For all subjects, the accuracies of four methods for testing set are shown in Fig. 8. We define the left hand movement and right hand movement as positive class and negative class, respectively. The ROC curves of four methods for testing set are shown in Fig. 9 (subject 2). According to Figs. 7–9, the average accuracy using CNN (86.41 ± 0.77%) is 9.24%, 3.80 and 5.16% higher than those using power + SVM (77.17 ± 7.69%),
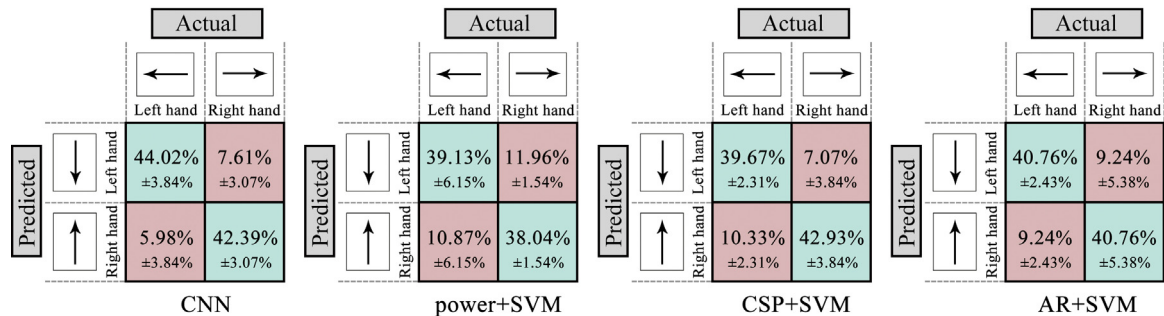

Fig. 7. Confusion matrices of four methods for testing set. The number of each entry in the matrix represents the mean value and standard deviation across all subjects. The main diagonal entries stand for the correct classification, and the off-diagonal entries stand for the misclassification.
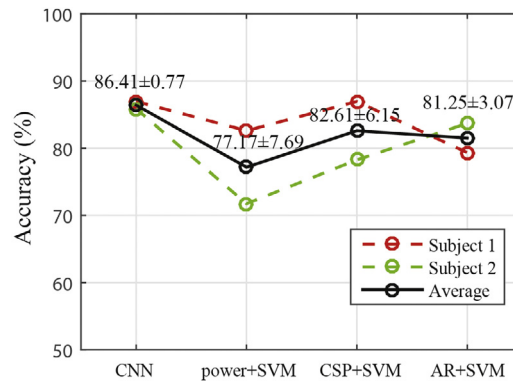
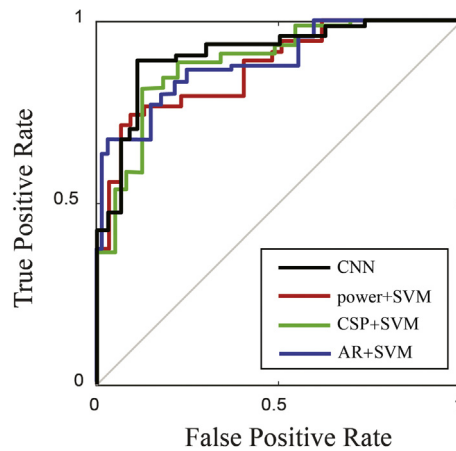**Fig. 8.** Accuracies of four methods for testing set.

Fig. 9. ROC curves of four methods for testing set (subject 2).

CSP + SVM (82.61 ± 6.15%) and AR + SVM (81.25 ± 3.07%), respectively. In addition, the AUC (area under curve) of the ROC curve of CNN is larger than those of the other three methods. These results demonstrate that CNN model has a better classification performance.

The precision, recall and *F*-score of the two classes using four methods are shown in Table 1. In general, the results showing high precision, recall and *F*-score indicate that the model has a high performance (CNN). To evaluate the *classification method × MI class* interaction and classification method and MI class, a 4 (CNN, power + SVM, CSP + SVM and AR + SVM) × 2 (left hand movement or right hand movement) within-subjects ANOVA is applied. All statistics used are carried out at 95% confidence interval. ANOVA shows no significant interaction between classification method and MI class ($p > 0.05$); there is a significant main effect of classification method ($F = 6.701$, $p = 0.001$) for the classification accuracy, while no significant main effect of MI class ($F = 0.002$, $p = 0.962$) for the classification accuracy.

Table 1
The precision, recall and *F*-score of the two classes using four methods.

		CNN		Power + SVM		CSP + SVM		AR + SVM	
		Left hand	Right hand	Left hand	Right hand	Left hand	Right hand	Left hand	Right hand
Subject 1	Precision	0.8269	0.9250	0.8000	0.8571	0.9048	0.8400	0.7647	0.8293
	Recall	0.9348	0.8043	0.8696	0.7826	0.8261	0.9130	0.8478	0.7391
	F-core	0.8776	0.8604	0.8333	0.8182	0.8636	0.8750	0.8041	0.7816
Subject 2	Precision	0.8837	0.8367	0.7273	0.7083	0.7955	0.7708	0.8780	0.8039
	Recall	0.8261	0.8913	0.6957	0.7391	0.7609	0.8043	0.7826	0.8913
	F-core	0.8539	0.8631	0.7111	0.7234	0.7778	0.7872	0.8276	0.8453

4. Conclusion

In this paper, we propose a new method based on the deep convolutional neural network (CNN) to perform feature extraction and classification for MI EEG signal. According to the spatio-temporal characteristics of EEG, a 5-layer CNN model is built to classify MI tasks (left hand and right hand). The results demonstrate that CNN can further improve classification performance compared with other three conventional methods. The present study shows that the proposed method is effective to classify MI, and provides a practical method by non-invasive EEG signal in BCI applications.

Acknowledgments

References

[1] N. Birbaumer, L.G. Cohen, Brain–computer interfaces: communication and restoration of movement in paralysis, J. Physiol. 579 (3) (2007) 621–636.
[2] B. Varkuti, C. Guan, Y. Pan, K.S. Phua, K.K. Ang, C.W.K. Kuah, K. Chua, B.T. Ang, N. Birbaumer, R. Sitaram, Resting state changes in functional connectivity correlate with movement recovery for BCI and robot-assisted upper-extremity training after stroke, Neurorehabil. Neural Repair 27 (1) (2013) 53–62.
[3] L.M. McCane, S.M. Heckman, D.J. McFarland, G. Townsend, J.N. Mak, E.W. Sellers, D. Zeitlin, L.M. Tenteromano, J.R. Wolpaw, T.M. Vaughan, P300-based brain–computer interface (BCI) event-related potentials (ERPS): People with amyotrophic lateral sclerosis (ALS) vs. age-matched controls, Clin. Neurophysiol. 126 (11) (2015) 2124–2131.
[4] I. Milovanovic, R. Robinson, E.E. Fetz, C.T. Moritz, Simultaneous and independent control of a brain–computer interface and contralateral limb movement, Brain Comput. Interfaces 2 (4) (2015) 174–185.
[5] E. Yin, Z. Zhou, J. Jiang, F. Chen, Y. Liu, D. Hu, A novel hybrid BCI speller based on the incorporation of SSVEP into the P300 paradigm, J. Neural Eng. 10 (2) (2013) 026012.
[6] M. Wang, I. Daly, B.Z. Allison, J. Jin, Y. Zhang, L. Chen, X. Wang, A new hybrid BCI paradigm based on P300 and SSVEP, J. Neurosci. Methods 244 (2015) 16–25.
[7] J.S. Brumberg, J.D. Burnison, K.M. Pitt, Using motor imagery to control brain–computer interfaces for communication, in: International Conference on Augmented Cognition, Springer, 2016, pp. 14–25.
[8] G. Pfurtscheller, F.L. Da Silva, Event-related EEG/MEG synchronization and desynchronization: basic principles, Clin. Neurophysiol. 110 (11) (1999) 1842–1857.
[9] M. Pregenzer, G. Pfurtscheller, Frequency component selection for an EEG-based brain to computer interface, IEEE Trans. Rehabil. Eng. 7 (4) (1999) 413–419.
[10] G. Pfurtscheller, Graphical display and statistical evaluation of event-related desynchronization (ERD), Electroencephalogr. Clin. Neurophysiol. 43 (5) (1977) 757–760.
[11] F. Lotte, M. Congedo, A. Lécuyer, F. Lamarche, B. Arnaldi, A review of classification algorithms for EEG-based brain–computer interfaces, J. Neural Eng. 4 (2) (2007) 1–24.
[12] N. Naseer, K.-S. Hong, FNIRS-based brain–computer interfaces: a review, Front. Hum. Neurosci. 9 (2015) 3.
[13] D. Ciregan, U. Meier, J. Schmidhuber, Multi-column deep neural networks for image classification, in: 2012 IEEE Conference on Computer Vision and Pattern Recognition (CVPR), IEEE, 2012, pp. 3642–3649.
[14] D. Huang, P. Lin, D.-Y. Fei, X. Chen, O. Bai, Decoding human motor activity from EEG single trials for a discrete two-dimensional cursor control, J. Neural Eng. 6 (4) (2009) 1–12.
[15] G. Pfurtscheller, C. Neuper, D. Flotzinger, M. Pregenzer, EEG-based discrimination between imagination of right and left hand movement, Electroencephalogr. Clin. Neurophysiol. 103 (6) (1997) 642–651.
[16] Y. LeCun, L. Bottou, Y. Bengio, P. Haffner, Gradient-based learning applied to document recognition, Proc. IEEE 86 (11) (1998) 2278–2324.
[17] Y. Bengio, Y. LeCun, et al., Scaling learning algorithms towards AI, Large-Scale Kernel Mach. 34 (5) (2007) 1–41.
[18] S. Sukittanon, A.C. Surendran, J.C. Platt, C.J. Burges, Convolutional networks for speech detection, in: Interspeech, Citeseer, 2004.
[19] H. Cecotti, A. Graser, Convolutional neural networks for P300 detection with application to brain–computer interfaces, IEEE Trans. Pattern Anal. Mach. Intell. 33 (3) (2011) 433–445.
[20] R.C. Oldfield, The assessment and analysis of handedness: the Edinburgh inventory, Neuropsychologia 9 (1971) 97–113.
[21] Y.A. LeCun, L. Bottou, G.B. Orr, K.-R. Müller, Efficient backprop, in: Neural Networks: Tricks of the Trade, Springer, 2012, pp. 9–48.
[22] Y. Park, L. Luo, K.K. Parhi, T. Netoff, Seizure prediction with spectral power of EEG using cost-sensitive support vector machines, Epilepsia 52 (10) (2011) 1761–1770.
[23] C. Liu, H.-b. Zhao, C.-s. Li, H. Wang, CSP/SVM-based EEG classification of imagined hand movements, J. Northeast. Univ. (Nat. Sci.) 8 (2010) 1098–1101.
[24] Y. Zhang, B. Liu, X. Ji, D. Huang, Classification of EEG signals based on autoregressive model and wavelet packet decomposition, Neural Process. Lett. (2016) 1–14.